



ELSEVIER

Contents lists available at ScienceDirect

## Deep-Sea Research I

journal homepage: [www.elsevier.com/locate/dsr](http://www.elsevier.com/locate/dsr)

## Instruments and Methods

## Application of underwater optical data to estimation of primary productivity

Makio C. Honda<sup>a,\*</sup>, Kosei Sasaoka<sup>b</sup>, Hajime Kawakami<sup>a</sup>, Kazuhiko Matsumoto<sup>a</sup>, Shuichi Watanabe<sup>a</sup>, Tommy Dickey<sup>c</sup><sup>a</sup> Mutsu Institute for Oceanography, Japan Agency for Marine-Earth Science and Technology, Yokosuka, Japan<sup>b</sup> Frontier Research Center for Global Change, Japan Agency for Marine-Earth Science and Technology, Yokohama, Japan<sup>c</sup> Ocean Physics Laboratory, Department of Geography, University of California, Santa Barbara, CA 93117, USA<sup>d</sup> Marine Technology Center, Japan Agency for Marine-Earth Science and Technology, Yokosuka, Japan

## ARTICLE INFO

## Article history:

Received 6 February 2009

Received in revised form

31 August 2009

Accepted 31 August 2009

## Keywords:

In situ optical sensor

Time-series observation

Primary productivity

North Pacific

Biological pump

## ABSTRACT

We conducted time-series observations of optical fields near the base of the euphotic zone (approximately 40 m) using moored automatic optical sensors at a time-series station in the Western Pacific Subarctic Gyre from March 2005 to July 2006 (with some gaps). We used the ratio of photosynthetically available radiation at the surface (surface PAR) to in situ quantum irradiance (in situ QI) at about 40 m as an index of opacity (surface PAR/in situ QI), which began to increase in the middle of April and peaked between the end of June and the middle of July 2005. This ratio then decreased toward winter. The ratio increased again beginning in January 2006, and large peaks were observed in June and July 2006. As an index of chlorophyll abundance we used the ratio of spectral irradiance at wavelengths of 555 and 443 nm ( $Ed_{555}/Ed_{443}$ ) at about 40 m; seasonal variability of this ratio synchronized well with the attenuation coefficient “*k*” estimated with surface PAR, in situ QI, and BLOOMS depth. We estimated primary productivity (PP) using  $Ed_{555}/Ed_{443}$  and an empirical equation based on a previous model but improved on the basis of shipboard observations. Estimated PP agreed well with observed PP. Seasonal variability of estimated PP was synchronized with that of organic carbon flux observed by sediment traps from approximately 150, 540, 1000, and 5000 m. This study demonstrates that time-series observations of in situ optical fields could contribute to the estimation of primary productivity and the study of the biological pump in the ocean.

© 2009 Elsevier Ltd. All rights reserved.

## 1. Introduction

Time-series observations of biogeochemical transformations are important for the quantitative verification of the ocean's role in the uptake of atmospheric CO<sub>2</sub>. Regular biogeochemical and physical time-series observations have been conducted using ships at a few sites in the world

ocean over the past two decades or longer (station ALOHA [e.g., Karl and Lukas, 1996; Karl et al., 2001], station BATS [e.g., Steinberg et al., 2001], Ocean Station Papa [OSP; e.g., Harrison, 2002]). However, frequent observations, even once per month, are insufficient for observing short-term events (e.g., Wiggert et al., 1994; Karl et al., 2001). Technological breakthroughs have enabled concurrent high-frequency, long-term biogeochemical and physical time-series observations by using moored systems with autonomous instrumentation (e.g., reviews by Dickey, 1991, 2001; Dickey and Falkowski, 2002; Kuwahara et al., 2003; review by Dickey et al., 2006). As part of the Joint Global

\* Corresponding author. present address: Marine Technology Center, Japan Agency for Marine-Earth Science and Technology, Yokosuka, Japan. Tel.: +81 46 867 9502; fax: +81 46 867 9375.

E-mail address: [hondam@jamstec.go.jp](mailto:hondam@jamstec.go.jp) (M.C. Honda).

Ocean Flux Study (JGOFS) and other related experiments, interdisciplinary moored systems were deployed off Bermuda (e.g., Dickey et al., 1998a, 2001), off Hawaii (e.g., Letelier et al., 2000), in the Arabian Sea (e.g., Dickey et al., 1998b), in the North Atlantic off Iceland (e.g., Dickey et al., 1994), in the equatorial Pacific (e.g., Foley et al., 1998; Chavez et al., 1999), in the Southern Ocean (Abbott et al., 2000), and in coastal environments (Taylor and Howes, 1994). These efforts have clearly demonstrated the efficacy of simultaneous high-frequency bio-optical and physical sampling over seasonal cycles to determine variability in phytoplankton biomass and its relationships with physical processes (see review by Dickey et al., 2006). Thus, new technologies are available to investigate important biological and biogeochemical processes at previously unsampled and unexplored temporal spectral ranges.

Time-series observation of primary productivity in the sunlit layer is essential for the study of the biological pump (Volk and Hoffert, 1985). Progress in satellite oceanography has undoubtedly enabled us to study large-scale spatial and temporal variation of biological activity and primary productivity in the upper ocean (Behrenfeld and Falkowski, 1997; Banse and English, 1999; Campbell et al., 2002; Behrenfeld et al., 2005; Dickey et al., 2006). However, ocean color data provide only near-surface information, and the presence of clouds and, sometimes, whitecaps often hampers the acquisition of satellite color data, especially in coastal and high-latitude regions.

Thus, we chose to observe and quantify biological activity—specifically, primary productivity—using in situ optical sensors moored in the euphotic layer. We have previously reported the estimation of primary productivity using in situ optical data and a proposed empirical model (Honda et al., 2006). This report improves our model by using a dataset from a longer period of observation (previous study, March–September 2005; this study, March 2005–July 2006 [with hiatus]) and by including more detailed considerations of each factor used in the empirical equation (integrated chlorophyll-*a* [Chl-*a*] concentration, satellite-derived photosynthetically available radiation [PAR], and light utilization index [ $\psi$ ]). An important component of this study was the measurement of primary productivity several times during the period of moored optical sensor operation between June and July 2006 using shipboard laboratory analysis methods. The primary productivity modeled in this study was directly compared with the observed primary productivity; thus, the accuracy of the model could be validated.

## 2. Methods

### 2.1. Mooring station and mooring system

Station K2 (47°N, 160°E; water depth approximately 5200 m) has been a time-series station in the Western Pacific Subarctic Gyre (WSG) since 2001, and seasonal observations have been conducted from research vessels (Kawakami and Honda, 2007; Kawakami et al., 2007) and

using mooring systems (Honda et al., 2006; Honda and Watanabe, 2007). The WSG is characterized by large seasonal variability in biogeochemical components such as  $p\text{CO}_2$  (Takahashi et al., 2002), surface nutrients (Louanchi and Najjar, 2000), and settling particles (Honjo, 1996; Honda et al., 2002), and by a more efficient biological pump than in other oceans (Honda, 2003; Buesseler et al., 2007, 2008; Special Issue of Deep-Sea Research II, vol. 55, 14–15, 2008).

Our bottom-tethered mooring system consisted of a water sampling system (McLane RAS-3-48-500), multiple time-series sediment traps (McLane Mark 7G-13 or 7G-21), and the Bio-optical Long-term Optical Ocean Measuring System (BLOOMS; described in Section 2.2). Results obtained using other instrumentation have been published elsewhere (Honda et al., 2006; Honda and Watanabe, 2007). The moored system with BLOOMS was deployed three times: March–September 2005, October 2005–May 2006, and June–July 2006.

### 2.2. Moored underwater optical sensor

The Bio-optical Long-term Optical Ocean Measuring System package (BLOOMS) consisted of a fluorometer (Wet Labs, Inc.), and a spectral radiometer (OCR-504-ICWS; Satlantic, Inc.) along with data acquisition/storage systems and a pressure housing (photograph in Chang et al., 2008). BLOOMS was mounted on the frame of the automatic water sampling system (McLane RAS-3-48-500; Honda and Watanabe, 2007), which was located at around 40 m water depth, for the measurement of Chl-*a* and downwelling spectral irradiance ( $E_d$ ) at four wavelengths (412, 443, 490, and 555 nm) on the hour from 0600 to 1800 local time (12 h). A depth sensor (RIGO RMD-500) was also mounted on the water sampling system, and BLOOMS depths were recorded every 120 min during the mooring deployment. The optical system was kept free of biofouling by the use of copper shutters (Dickey et al., 2003; details in Manov et al., 2004). Unfortunately the fluorometer malfunctioned so we cannot present time-series data of fluorometric Chl-*a* from this study. The  $E_d$  at four wavelengths was measured every hour during local daytime periods (0600–1800 local time) from 20 March 2005 to 15 July 2006 (with some gaps).

Following equation (1) of Siegel et al. (2001), the daily quantum irradiance spectra over a wavelength (412–555 nm) and time ranges (12 h from 6:00 to 18:00 local time) (in situ QI:  $\text{quanta m}^{-2} \text{day}^{-1}$ ) was calculated by integrating  $E_d$  at four wavelengths and approximate daylight hours as follows:

$$\text{in situ QI} = \int_{412}^{555} \int_{6:00}^{18:00} (\lambda_{\text{ave}}/hc) E_d dt d\lambda \quad (1)$$

where  $\lambda_{\text{ave}}$  is the average of continuous wavelengths,  $h$  is Planck's constant and  $c$  is the velocity of light. The factor [ $\lambda_{\text{ave}}/hc$ ] accounts for conversion of an energy flux to quantum flux. Between about 20 March and 25 September, the local daylight period was longer than 12 h (with a maximum of 16 h around mid-June), and our calculated in situ QI values should be potentially underestimated.

relative to the actual daily values. However, we believe that the magnitude of the underestimate was at most 2% of in situ QI values on the basis of an empirical equation of diurnal change in PAR (e.g., Ikusima, 1967) and, thus, negligible for the purposes of our discussion.

### 2.3. Primary productivity and measurement of chlorophyll-*a* concentrations

During mooring servicing cruises for recovery and deployment of the BLOOMS mooring, primary productivity and Chl-*a* were measured using ship-based laboratory analysis methods. Instead of the  $^{14}\text{C}$  method (Stemann Nielsen, 1952; Marra and Barber, 2004), primary productivity was measured by the in situ  $^{13}\text{C}$  method developed by Hama et al. (1983). Water samples were collected with CTD/Carousel Water Sampling System (CTD: Sea-Bird 9plus, and 12-litter Niskin Bottles  $\times$  36) from the surface and seven predetermined depths corresponding to nominal specific optical depths, that is, approximately 50%, 25%, 10%, 5%, 2.5%, 1%, and 0.5% of surface PAR. All water samples used for primary productivity measurements (volume, 1 L) were spiked with  $\text{NaH}^{13}\text{CO}_3$  solution to a final concentration of  $200\ \mu\text{mol L}^{-1}$ , and then Nalgen polycarbonate bottles were attached at the appropriate depths on a drifting incubation system consisting of a 200-m line supported by floats at the surface and kept vertical by weights at the bottom. After 24-h in situ incubations, primary productivity samples were filtered through pre-combusted Whatman GF/F filters. Before analysis of the material on the filters, inorganic carbon was removed by an acid treatment in an HCl vapor bath for 4–5 h. The  $^{13}\text{C}$  content of samples was measured with a mass spectrometer system on board (ANCA-SL; PDZ Europe), and the amount of organic carbon assimilated and the primary productivity were calculated following Hama et al. (1983). The analytical method for  $^{13}\text{C}$  is more complicated (using mass spectrometry instead of liquid scintillation counter for  $^{14}\text{C}$ ), and there is a possibility that 24-h incubation with  $^{13}\text{C}$  might lose more extracellular metabolites (DOC) compared with a few to several hours incubation with  $^{14}\text{C}$ . However, Hama et al. (1983) reported that there is little difference between PP measured by  $^{14}\text{C}$  and  $^{13}\text{C}$  methods. Based on duplicate incubations for respective depths and stations during scientific cruises MR06-03 (June–July 2006), MR07-05 (September–October 2007), and MR08-05 (October–November 2008) using the same incubation techniques, the mean repeatability of our primary productivity measurements was better than 5% ( $n=104$ ).

Water samples for the measurement of Chl-*a* (0.5 L) were collected from nine layers in the upper 200 m. Water samples were vacuum filtered ( $<15\ \text{cmHg}$ ) through 25-mm diameter GF/F filters. Phytoplankton pigments retained on the filters were immediately extracted in a polypropylene tube with 7 mL of *N,N*-dimethylformamide (Suzuki and Ishimaru, 1990). The tubes were stored at  $-20^\circ\text{C}$  under dark conditions for 24 h or more to extract Chl-*a*. The fluorescence of each sample was measured using a fluorometer (model 10-AU-005; Turner Designs)

that had been previously calibrated against pure Chl-*a* (Sigma Chemical Co.). We used the fluorometric “acidification method” described by Holm-Hansen et al. (1965). Measurement error was approximately 3%. The total amount of Chl-*a* in the upper 60 m (Chl- $a_{(\text{int})}$ ; see Section 4.1) was estimated with integration of Chl-*a* upper 60 m at six layers (0, 10, 20, 30, 50, and 60 m) by the trapezoidal rule.

### 2.4. Underwater light conditions

Vertical profiles of underwater light conditions in the upper 100–200 m were measured during cruises with a profiling radiometer (Sea-viewing Wide Field-of-view Sensor [SeaWiFS]) Profiling Multichannel Radiometer [SPMR; Satlantic, Inc.). Descending gravitationally in the water column with sinking velocity of approximately  $1\ \text{m s}^{-1}$ , this profiler measures upwelling radiance ( $L_u$ ) and downwelling irradiance ( $E_d$ ) at 13 wavelengths from 380 to 705 nm. The relative intensity of solar irradiance in the water column was determined by comparison with surface PAR observed on deck by a SeaWiFS Multichannel Surface Reference (SMSR; Satlantic, Inc.). The observed irradiance data were used to determine the appropriate water sampling depths for measurements of primary productivity and for verification of the relative attenuation of irradiance at various wavelengths, especially the ratio of irradiance at a wavelength of 555 nm to that at 443 nm ( $E_{d555}/E_{d443}$ ) at around 40 m (see Section 4.1).

### 2.5. Surface PAR

Daily surface PAR data at station K2 were obtained from SeaWiFS satellite optical data. Clouds over station K2 often hampered the daily acquisition of PAR data there, so we compiled daily PAR data from an  $11 \times 11$  pixel box on the digital satellite data image (an area roughly  $100\ \text{km} \times 100\ \text{km}$ ) centered on station K2. As a result, daily surface PAR data were available for approximately 95% of the 499 days between 20 March 2005 and 31 July 2006. However, it is noted that the satellite-based daily surface PAR in any pixel was based on one or two “snapshots” obtained during daytime. In addition, satellite-based daily PAR did not always accurately represent that at station K2. Standard deviation of satellite PAR data ranged from less than 5% to 85% with average of  $\sim 20\%$ . Standard deviation tended to increase as surface PAR decreased and sometimes exceeded 100%. Based on a comparison of satellite-based PAR with PAR measured on deck during cruise MR06-03, we corrected for the differences between in situ and satellite-based PAR before estimating PP (see Section 4.2).

## 3. Results

Satellite-based surface PAR varied widely from day to day (Fig. 1a). In general, surface PAR increased from March 2005 toward June and July 2005 and then decreased toward winter, when the minimum surface PAR was observed, in December 2005. Surface PAR increased again

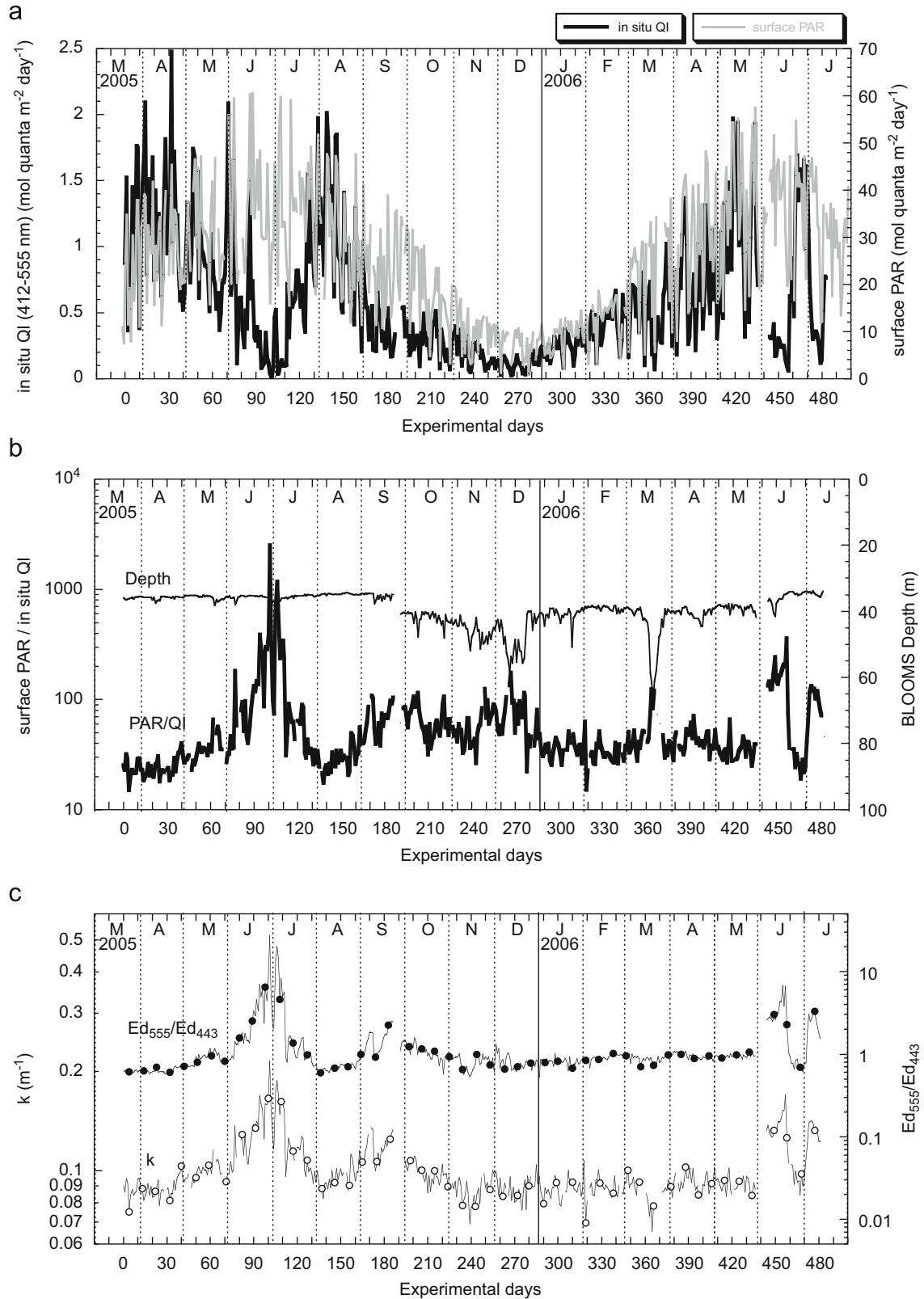


**Fig. 1.** Seasonal variability in (a) quantum irradiance at the depth of BLOOMS (in situ QI; heavy line) and surface PAR obtained from SeaWiFS data (surface PAR; gray line), (b) the noontime ratio of surface PAR to in situ QI (surface PAR/in situ QI) and BLOOMS depth, and (c) attenuation coefficient “ $k$ ” and the ratio of quantum irradiance at a wavelength of 555 nm to that at 443 nm ( $\text{Ed}_{555}/\text{Ed}_{443}$ ) at BLOOMS depths from March 2005 to July 2006. Experimental “day 0” is 20 March 2005. Note logarithmic scales for surface PAR/in situ QI (b), and “ $k$ ” and  $\text{Ed}_{555}/\text{Ed}_{443}$  (c). In order to understand seasonal variability easily, error bars are not shown (error bars are explained in the text).

thereafter, and maximum surface PAR was observed in late June 2006. In situ QI observed by BLOOMS also fluctuated widely (Fig. 1a). Overall, the fluctuations and seasonal variability synchronized well with surface PAR. However in situ QI decreased relative to surface PAR in June and July of 2005 and 2006.

As a result, the ratio of surface PAR to in situ QI (PAR/QI) increased in June and July 2005 and 2006 (Fig. 1b). If the depth of BLOOMS is constant, the PAR/QI ratio can serve as an index of the degree to which irradiance is attenuated, that is, index of opacity. During the first mooring deployment (March–September 2005) the depth of BLOOMS was stable and averaged approximately 35 m (Fig. 1b). However, during the second mooring (October 2005–May 2006) the depth of BLOOMS was fairly variable and slightly deeper, averaging approximately 40 m. The BLOOMS depth in December 2005 and March 2006 sometimes exceeded 60 m. The increase in the PAR/QI ratio in June and July of 2005 and 2006 without an increase in the deployment depth likely indicates an increase of opacity in the water column above BLOOMS.

In general, the magnitude of light attenuation in the water (attenuation coefficient “ $k$ ”) can be expressed following the Lambert–Beer law, which can be generally applied to ocean water (Gordon, 1989):

$$k = -\ln(I_z/I_0)/z \quad (2)$$

where  $I_z$  and  $I_0$  are downwelling irradiances at  $z$  and 0 m, respectively.

Although in situ  $QI_{(412-555)}$  does not cover all wavelengths for PAR (400–700 nm), substituting in situ  $QI_{(412-555)}$  and surface PAR with  $I_z$  and  $I_0$ , respectively, the attenuation coefficient “ $k$ ” was estimated (Fig. 1c). The “ $k$ ” increased in the late June and early July in 2005, and in June and early July in 2006. In addition, a small increase was observed in September 2005. Thus we suspect that, during the above period, the opacity in the water column above BLOOMS increased.

Seasonal variability in the noontime  $Ed_{555}/Ed_{443}$  ratio was well synchronized with that in “ $k$ ”, which increased in late June–early July 2005, in June 2006 and in July 2006 (Fig. 1c). We also observed a small the  $Ed_{555}/Ed_{443}$  ratio in late September 2005 similarly to “ $k$ ”. As described in Section 4.1, the increases of “ $k$ ” and the  $Ed_{555}/Ed_{443}$  ratio were attributed to increases of phytoplankton.

## 4. Discussion

### 4.1. Estimation of depth-integrated Chl- $a$

In clear oceanic water, the magnitude of extinction of downwelling irradiance at approximately 550 nm ( $Ed_{550}$ , green light) is larger than that at approximately 440 nm ( $Ed_{440}$ , blue light) (e.g., Kirk, 1983), that is, “ $k$ ” for  $Ed_{555}$  ( $k_{555}$ ) is larger than “ $k$ ” for  $Ed_{444}$  ( $k_{444}$ ). However,  $k_{444}$  increases when particulate materials increases. This is attributed mainly to the fact that  $Ed_{440}$  is preferentially absorbed by Chl- $a$ , the main photosynthetic pigment of the principal phytoplankton groups such as diatoms and

coccolithophorids, as opposed to  $Ed_{550}$  (e.g., Kirk, 1983; Vaillancourt et al., 2003). Duntley et al. (1974) and Gordon and Morel (1983) reported a good correlation between Chl- $a$  concentrations and  $Ed_{441}$ , but no correlation with  $Ed_{520}$ . Smith et al. (1991) and Abbott et al. (1995) documented a good relationship between Chl- $a$  and the  $Ed_{441}/Ed_{520}$  ratio. Loisel and Morel (1998) and Kinkade et al. (2001) also reported a good correlation between depth-integrated Chl- $a$  ( $Chl-a_{int}$ ) over the upper 65 m of the water column and the  $Ed_{443}/Ed_{550}$  ratio from noon measurements at 65 m depth. Furthermore, Abbott et al. (2000) showed that there was a good relationship between  $Chl-a_{int}$  and the ratio of  $Ed_{443}$  to  $Ed_{555}$  but not to  $Ed_{520}$  or  $Ed_{550}$ .

We compared estimates of  $Chl-a_{int}$  in the upper 60 m of the water column, which is the approximate annual maximum depth of the euphotic layer at station K2 (Imai et al., 2002; Honda, in preparation), to  $Ed_{555}/Ed_{443}$  at 40 m (Fig. 2). These values for  $Ed_{555}/Ed_{443}$ , the reciprocal of  $Ed_{443}/Ed_{555}$ , were collected by an underwater SPMR optical vertical profiler during multiple scientific cruises in the northern North Pacific (R/V *Mirai*, *Natsushima*, and *Kairei* cruise reports from 2003 to 2008). Note that we are investigating the relationship between  $Ed_{555}/Ed_{443}$  at 40 m and the  $Chl-a_{int}$  in the upper 60 m, not 40 m. The depth of 60 m is the approximate annual maximum depth of the euphotic layer in the WSG, and primary productivity is often conducted below 40 m. Moreover, light utilization index

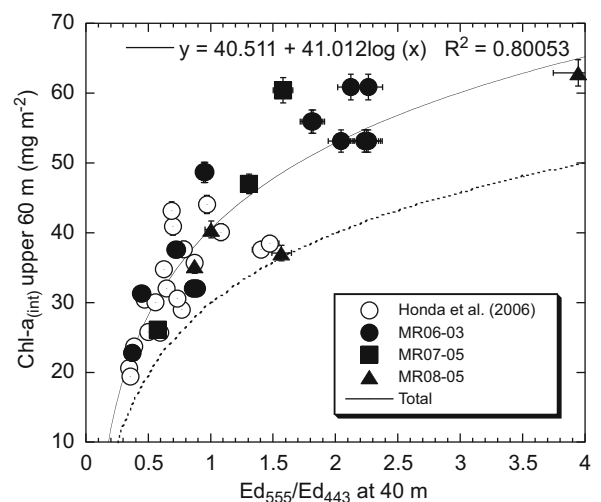


**Fig. 2.** The relationship between  $Ed_{555}/Ed_{443}$  at a depth of 40 m and integrated chlorophyll- $a$  concentrations in the upper 60 m ( $Chl-a_{int}$ ).  $Ed_{555}/Ed_{443}$  was determined by profiling radiometer (see Section 2.4), and chlorophyll- $a$  concentrations were determined by fluorometer (see Section 2.3). Open circles represent data from various locations in the northern North Pacific during cruise MR05-04 (September–October 2005) and previous cruises in various seasons (see Honda et al., 2006 for details). Closed circles, squares, and triangles represent data from research cruises MR06-03 (June–July 2006), MR07-05 (September–October 2007), and MR08-05 (October–November 2008), respectively. The solid line indicates the regression curve based on all data. Error bars are one standard deviation ( $1\sigma$ ). Broken line is relation between  $Ed_{555}/Ed_{443}$  at 40 m and  $Chl-a_{int}$  upper “40 m” reported previously (Honda et al., 2006).

( $\Psi$ , see below) was estimated with primary productivity and Chl- $a$  below 40 m. Thus a previous study showed that Chl- $a_{\text{int}}$  in the upper 40 m was likely insufficient for the estimation of primary productivity in the water column (Honda et al., 2006). We found a good correlation between  $\text{Ed}_{555}/\text{Ed}_{443}$  at 40 m and Chl- $a_{\text{int}}$  over the upper 60 m ( $r^2 > 0.8$ ,  $P < 0.001$ ; Fig. 2), although these data were obtained during different seasons and from different places in the subarctic North Pacific (Honda et al., 2006 and references in caption to Fig. 2). As a result, the Chl- $a_{\text{int}}$  over the upper 60 m can be estimated from the  $\text{Ed}_{555}/\text{Ed}_{443}$  ratio at 40 m as follows:

$$\text{Chl} - a_{\text{int}}(\text{mg m}^{-2}) = 41.01 \log(\text{Ed}_{555}/\text{Ed}_{443}) + 40.51 \quad (3)$$

As seen in Fig. 2, estimated Chl- $a_{\text{int}}$  in the upper 60 m is approximately  $65 \text{ mg m}^{-2}$  and approximately 30% larger than Chl- $a_{\text{int}}$  in the upper 40 m ( $50 \text{ mg m}^{-2}$ ) when the  $\text{Ed}_{555}/\text{Ed}_{443}$  ratio at 40 m is 4.

It is noted that  $\text{Ed}_{555}/\text{Ed}_{443}$  ratios were not always observed by BLOOMS at 40 m, but at variable depth (Fig. 1b). The relation between  $\text{Ed}_{555}/\text{Ed}_{443}$  at 40 m and that at variable depths (35–60 m) was investigated with SPMR data, and it was recognized that  $\text{Ed}_{555}/\text{Ed}_{443}$  ratios vary with depth (Fig. 3). As a whole,  $\text{Ed}_{555}/\text{Ed}_{443}$  decreased with depth. This is likely attributable to the fact that  $k_{555}$  is generally larger than  $k_{443}$  as described above. However  $\text{Ed}_{555}/\text{Ed}_{443}$  sometimes increased with depth, or increased and decreased between 35 and 60 m. In addition, the magnitude of change with depth was variable. Gordon (1989) reported that the “ $k$ ” value is not constant in the water column and varies with depth. However, based on average and standard deviation of relative  $\text{Ed}_{555}/\text{Ed}_{443}$  at

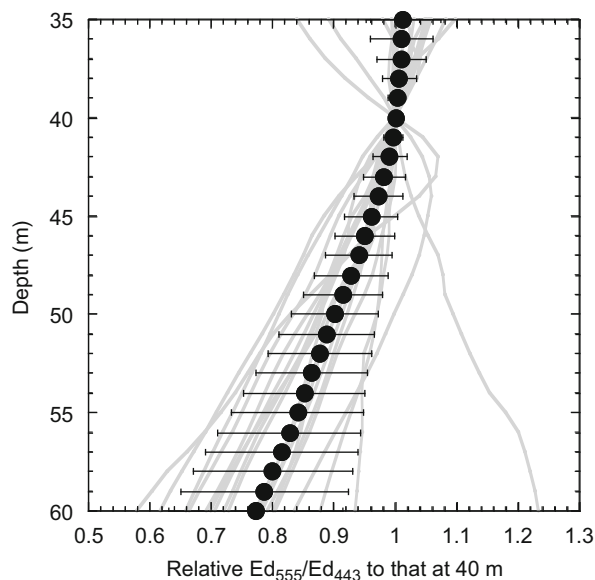


**Fig. 3.** Vertical profiles of relative  $\text{Ed}_{555}/\text{Ed}_{443}$  at various depths between 35 and 60 m to  $\text{Ed}_{555}/\text{Ed}_{443}$  at 40 m observed with profiling radiometer during various cruises (gray lines). Closed circles and error bars are average of relative  $\text{Ed}_{555}/\text{Ed}_{443}$  and standard deviations at various depths, respectively.

respective depths (Fig. 3), the following trend can be found.

- (i) Between 35 and 60 m,  $\text{Ed}_{555}/\text{Ed}_{443}$  decreases with depth linearly, but this slope is different above 40 m than it is 40 m.
- (ii) Standard deviation (that is, error) of  $\text{Ed}_{555}/\text{Ed}_{443}$  at respective depth increases with distance from 40 m.

We propose empirical equations for relative  $\text{Ed}_{555}/\text{Ed}_{443}$  and standard deviation (error) at respective depth ( $z$  m) to that at 40 m (Relative  $\text{Ed}_{555}/\text{Ed}_{443}(z)$  and  $\text{SD}(z)$ ) as follows:

$$(\lt 40 \text{ m}) \quad \text{Relative } \text{Ed}_{555}/\text{Ed}_{443}(z) = -0.002z + 1.097 \quad (4)$$

$$\text{SD}(z) = -0.012z + 0.471 \quad (40 - 60 \text{ m}) \quad (5)$$

$$\text{Relative } \text{Ed}_{555}/\text{Ed}_{443}(z) = -0.012z + 1.487 \quad (6)$$

$$\text{SD}(z) = 0.007z - 0.255 \quad (7)$$

For example,  $\text{Ed}_{555}/\text{Ed}_{443}$  at 50 m (60 m) is estimated to be  $0.90 \pm 0.07$  ( $0.78 \pm 0.14$ ) of  $\text{Ed}_{555}/\text{Ed}_{443}$  at 40 m. Thus, using these empirical equations, we corrected (or normalized)  $\text{Ed}_{555}/\text{Ed}_{443}$  observed at variable depths to that at 40 m. After that, by using Eq. (3), we estimated the seasonal variability in Chl- $a_{\text{int}}$ . The total error of Chl- $a_{\text{int}}$  from error of estimation of  $\text{Ed}_{555}/\text{Ed}_{443}$  at 40 m ( $\sim 4\%$  on average) and Eq. (3) ( $\sim 20\%$  on average) was approximately 22% on average. It is noted that the attenuation coefficient “ $k$ ” (Fig. 1c) correlated well with Chl- $a_{\text{int}}$  ( $r^2=0.82$ ).

#### 4.2. Estimation of primary productivity

The optical information obtained by BLOOMS provides a means for the estimation of primary productivity. Using

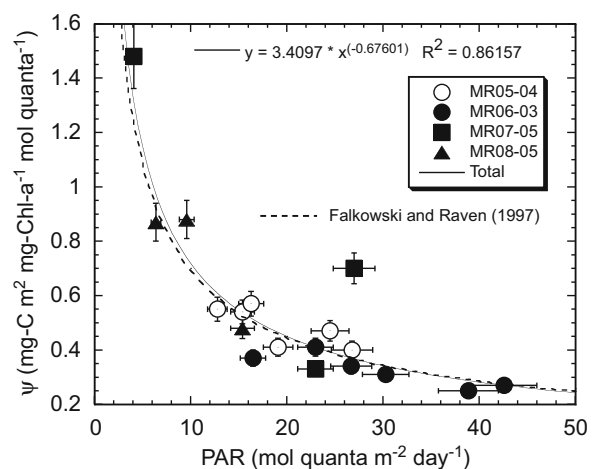


**Fig. 4.** The relationship between light utilization index ( $\Psi$ ) and surface PAR as observed on deck. Open circles represent data from various locations in the northern North Pacific during cruise MR05-04. Closed circles, squares, and triangles indicate data from cruises MR06-03, MR07-05, and MR08-05, respectively. The solid line indicates the regression curve based on all data. Broken line is regression curve proposed on Fig. 9.9 in Falkowski and Raven (1997).

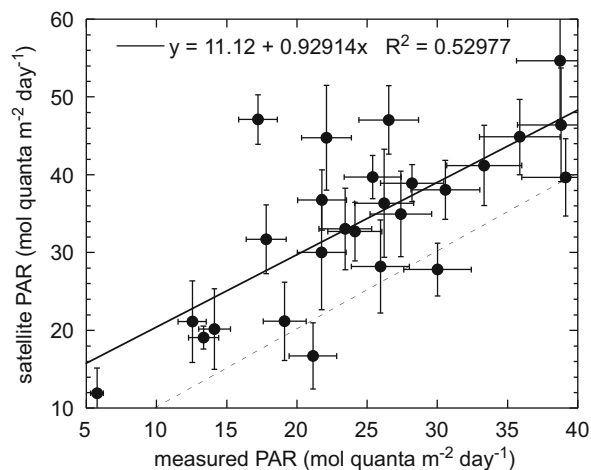


**Fig. 5.** A comparison of surface PAR measured onboard (measured PAR) and surface PAR obtained from SeaWiFS (satellite PAR). The solid line is the regression line, and the broken line indicates  $y=x$  (satellite PAR=measured PAR). Vertical error bars are one standard deviation for satellite PAR. Horizontal bar is official accuracy of surface PAR (8%).

the following empirical Eq. (8), depth-integrated primary productivity in the euphotic layer (PP) can be determined from the  $\text{Chl-}a_{\text{int}}$ , estimated as described in Section 4.1, and the daily surface PAR obtained by SeaWiFS:

$$\text{PP} = \text{Chl-}a_{\text{int}} \times \text{surface PAR} \times \Psi \quad (8)$$

where  $\Psi$  is the water column light utilization index (or efficiency) ( $\text{mg-C m}^2 \text{ mg-chl-}a^{-1} \text{ mol quanta}^{-1}$ ). Falkowski (1981) defined  $\Psi$  as the ratio of  $\text{Chl-}a_{\text{int}}$  specific productivity to surface PAR. Platt (1986) and Platt et al. (1988) reported a relatively constant  $\Psi$  (approximately  $0.4 \text{ mg-C m}^2 \text{ mg-chl-}a^{-1} \text{ mol quanta}^{-1}$ ) on regional and global scales, whereas Falkowski and Raven (1997) reported that  $\Psi$  increases with decreasing light intensity (PAR). In contrast, Shiomoto (2000) reported an increase of  $\Psi$  with increasing PAR, attributing this to the effects of the spring bloom. Hashimoto and Shiomoto (2002) found that  $\Psi$  ranged from 0.3 to  $1.2 \text{ mg-C m}^2 \text{ mg-chl-}a^{-1} \text{ mol quanta}^{-1}$ , and large-sized phytoplankton (diatoms) tended to have a higher  $\Psi$  based on spring and summer observations in the western and eastern North Pacific. In

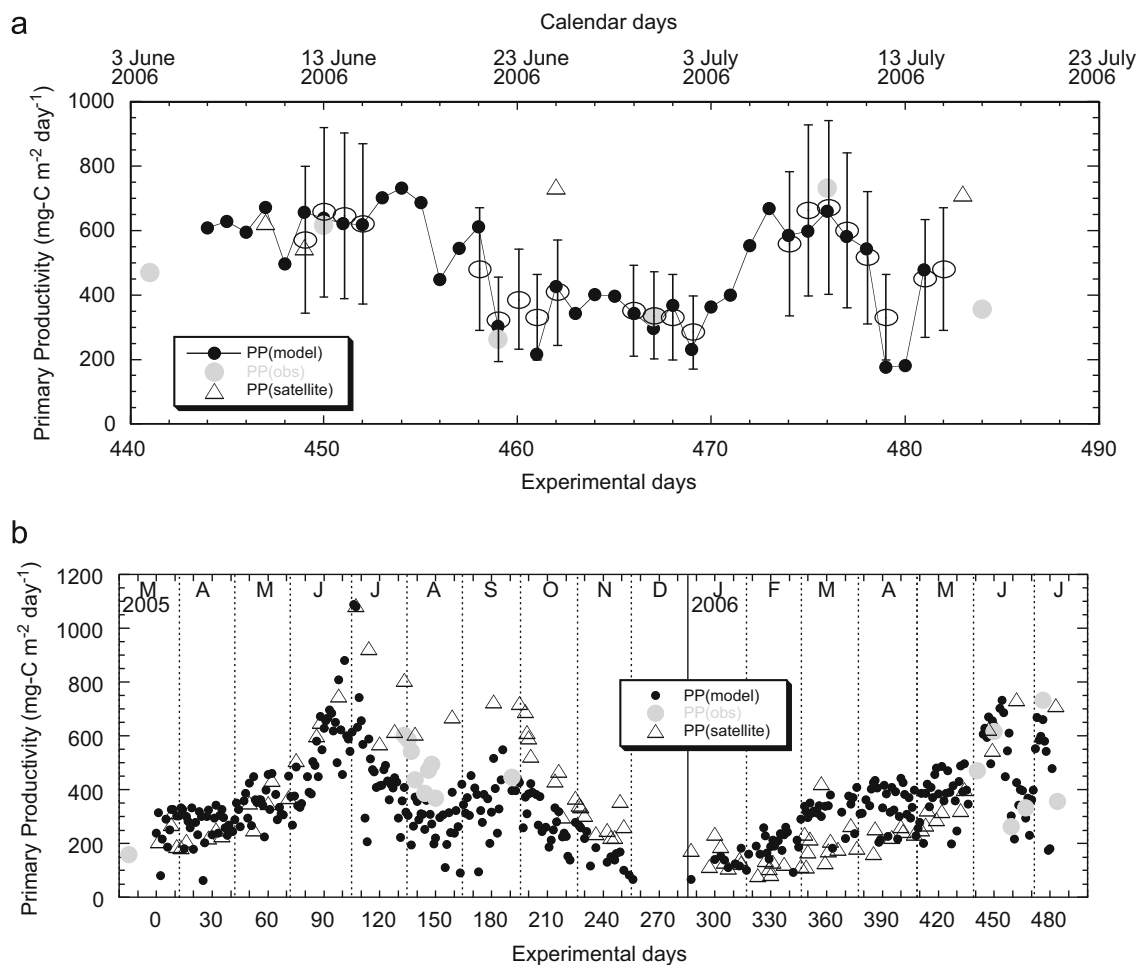


**Fig. 6.** Primary productivity (PP) estimated from BLOOMS data and empirical equations from this study ( $\text{PP}_{\text{(model)}}$ , closed circles), PP measured onboard using the in situ incubation method with  $^{13}\text{C}$  ( $\text{PP}_{\text{(obs)}}$ , gray circles) and PP estimated from satellite data and an algorithm (Behrenfeld and Falkowski, 1997) ( $\text{PP}_{\text{(satellite)}}$ , open triangles) (a) during cruise MR06-03 (June–July 2007) and (b) from March 2005–July 2006. Observed PP data during late July and August 2005 are from Boyd et al. (2008). In (a), modeled PP estimated with onboard PAR are also shown (open circles). Although error bars for these data (40% on average) are shown, error bars for modeled PP estimated with satellite PAR are not shown in order to understand variability in modeled PP and compare with observed PP easily.

contrast, Imai et al. (2002) reported that  $\Psi$  was constant throughout the year at time-series station KNOT in the WSG ( $0.3 \pm 0.1 \text{ mg-C m}^{-2} \text{ mg-chl-}a^{-1} \text{ mol quanta}^{-1}$ ).

Using data from our recent cruises in the northern North Pacific (MR05-04 [September–October 2005], MR06-03, MR07-05, and MR08-05), we calculated  $\Psi$  values on the basis of primary productivity, Chl-*a* and surface PAR values measured on board in the northern North Pacific, including stations in the Bering Sea and in the eastern North Pacific (at OSP). The  $\Psi$  values ranged from 0.2 to 1.5 with error of approximately 8% (Fig. 4). We analyzed the relationship between  $\Psi$  values and surface seawater temperature (SST), Chl-*a*<sub>int</sub>, surface nutrient (NO<sub>3</sub>) and surface PAR, and found that the  $\Psi$  values were significantly correlated with surface PAR ( $r^2 > 0.86$ ,  $P < 0.0001$ ) and tended to decrease with increasing surface PAR (Fig. 4). The power function proposed here coincided well with the relation between  $\Psi$  and surface PAR reported by Falkowski and Raven (1997). As their relation was obtained from a large amount of data in the world ocean while our data were from only the northern North Pacific, this relation can be applied to the world ocean. Though we cannot explain whether it is due to physiological adaptations to low light or to some other factor,  $\Psi$  was determined using the following power function in this study:

$$\Psi = 3.41(\text{surface PAR})^{-0.68} \quad (9)$$

Before we estimated primary productivity, we first determined the validity of the daily surface PAR from satellite observations (satellite-based PAR), although in our previous study (Honda et al., 2006) satellite-based PAR was used without any validation. During the MR06-03 cruise, satellite-based PAR was compared with the daily surface PAR measured onboard with a hyperspectral UV–VIS irradiance sensor (RAMSES-ACC, TriOS Optical Sensors; observed wavelengths: each 1 nm wavelength between 400 and 700 nm, sampling time: each 5 min, official accuracy: better than 6–10%). As a result, we found that satellite-based PAR tended to be higher than the onboard PAR (Fig. 5). As mentioned previously (Section 2.5), satellite-based PAR is an average daily PAR over a  $100 \text{ km} \times 100 \text{ km}$  area ( $11 \times 11$  pixels centered on station K2) and daily PAR for each pixel is based on only a few data points. When the surface PAR at station K2 was too low to be detected, the detectable surface PAR from the surrounding area was used to represent surface PAR at station K2. This arithmetic processing might tend to make values of satellite-based PAR higher than the onboard or actual surface PAR. Although the correlation between measured and satellite PAR was low (but significant; see Fig. 5), satellite-based surface PAR values were corrected in this study as follows:

$$\text{Surface PAR} = 1.075 \text{ satellite-based PAR} - 11.957 \quad (10)$$

$(n = 26, r^2 = 0.53, p < 0.0001)$

Thus, primary productivity during MR06-03 (June and July 2006) was estimated using Ed<sub>555</sub>/Ed<sub>443</sub> data obtained by BLOOMS, corrected satellite-based surface PAR, and Eqs. (3)–(9) (Fig. 6a). The total uncertainty in PP estimated with onboard PAR was approximately 40% on average

(Fig. 6a). On the other hand, the total uncertainty in PP estimated with satellite-based and corrected PAR was larger than 100% on average because the error (standard deviation) of  $\Psi$  estimated with surface PAR, whose error was  $\sim 52\%$  on average, exceeds 100%. Accurate measurement of surface PAR is a high-priority issue in the future. Estimated PP (hereafter: “modeled PP”) during June and July 2006 ranged from approximately 180 to  $730 \text{ mg-C m}^{-2} \text{ day}^{-1}$  (Fig. 6a). Although there were only four sets of modeled and observed PP data that were obtained on the same day, the modeled PP agreed well with observed PP (Fig. 6a). The period at station K2 under discussion—June and July—is usually very productive (e.g., Kawakami and Honda, 2007). However, onboard salinity and nutrient observations during cruise MR06-03 indicated that non-productive water invaded station K2 around early July 2006 (around experimental day 460). This low-production phenomenon is clearly represented in the modeled PP (Fig. 6a).

We used our model to estimate primary productivity for approximately a year and a half (March 2005–July 2006; Fig. 6b). Modeled PP in March 2005 and in late September 2005 also coincided well with observed PP. Although modeled PP tended to be slightly lower than observed PP in summer (late July and August 2005; reported by Boyd et al., 2008), the modeled PP reproduced an observed decrease of PP with time. The annual average of PP (20 March 2005–19 March 2006) was estimated at approximately  $350 \text{ mg-C m}^{-2} \text{ day}^{-1}$ . This estimate is within the range of previous annual estimates in the WSG: at station KNOT ( $270 \text{ mg-C m}^{-2} \text{ day}^{-1}$ ; Imai et al., 2002) and station K2 ( $350 \text{ mg-C m}^{-2} \text{ day}^{-1}$ ; MR08-05 preliminary cruise report, 2008).

We also estimated PP using satellite-based Chl-*a*, surface PAR, and SST data, and with the proposed algorithm (Vertical Generalized Production Model, VGPM,

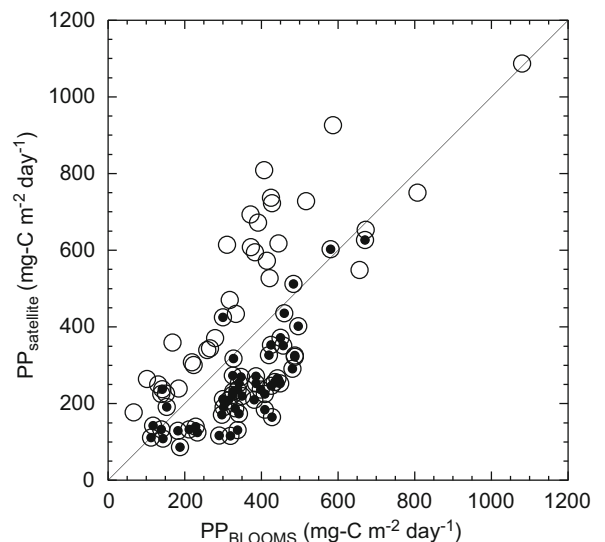
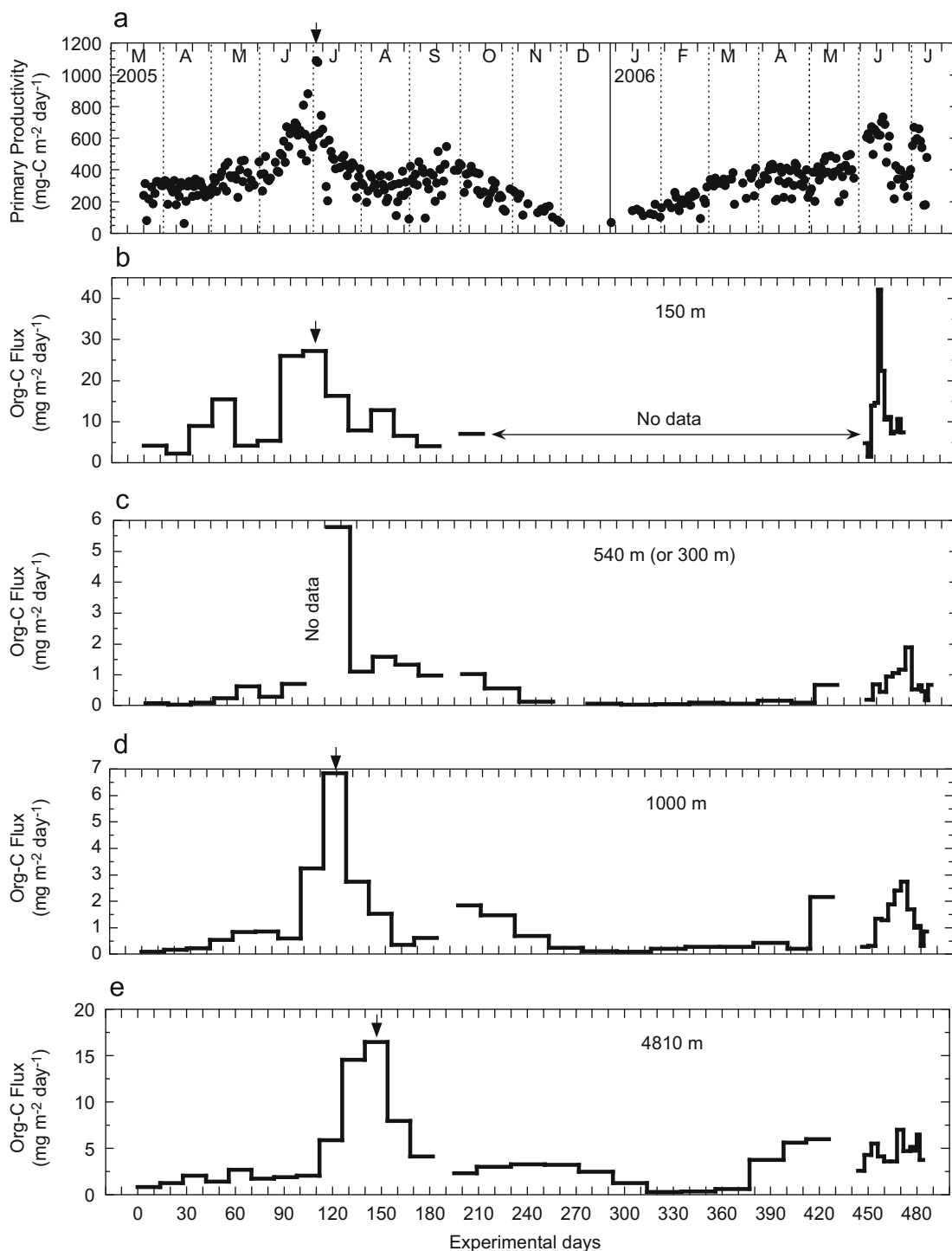


Fig. 7. Comparison of PP modeled with BLOOMS data and empirical equations from this study ( $PP_{\text{BLOOMS}}$ ) and PP estimated from satellite data and an algorithm ( $PP_{\text{satellite}}$ ). Solid line indicates  $y=x$ . Double circles are  $PP_{\text{satellite}}$  estimated with low SST ( $< 5^\circ\text{C}$ ).

Behrenfeld and Falkowski [1997]) (Fig. 6a and b). During June and July 2006, we were able to calculate satellite-based PP ( $PP_{\text{satellite}}$ ) for only four days (Fig. 6a).  $PP_{\text{satellite}}$  for the first 2 days agreed with modeled PP ( $PP_{\text{BLOOMS}}$ ) and observed PP. However, the other two  $PP_{\text{satellite}}$  were much

higher than  $PP_{\text{BLOOMS}}$ . From an annual perspective,  $PP_{\text{satellite}}$  and its seasonal variability coincided well with  $PP_{\text{BLOOMS}}$  between late May and mid-July 2005 (Fig. 6b). In contrast,  $PP_{\text{satellite}}$  between August 2005 and January 2006 tended to be higher than  $PP_{\text{BLOOMS}}$  and observed PP.



**Fig. 8.** Seasonal variability in (a) modeled PP (this study), and organic carbon fluxes observed by time-series sediment traps at (b) 150 m, (c) 540 m (or 300 m), (d) 1000 m, and (e) 4810 m (Honda, in preparation). Note that vertical scales for organic carbon flux are different for each depth. Arrows at respective depths are periods when large PP or organic carbon flux appeared (middle day of collecting period for sediment trap).

In addition, increases in  $PP_{\text{satellite}}$  were not obvious until after May 2006, whereas  $PP_{\text{BLOOMS}}$  began to increase in February 2006. There was a tendency for  $PP_{\text{satellite}}$  to be lower (higher) than  $PP_{\text{BLOOMS}}$  during January and May (during June and December) when SST is lower (higher) than 5 °C (Fig. 7). In VGPM, the maximum chlorophyll-specific PP in the water column ( $P_{\text{opt}}^B$ ) is one of the key parameters, and  $P_{\text{opt}}^B$  is defined as a “seventh degree function of SST”. However, this  $P_{\text{opt}}^B$  has large uncertainty (Behrenfeld and Falkowski, 1997). Thus  $P_{\text{opt}}^B$  under temperature lower (higher) than 5 °C might be underestimated (overestimated), resulting in an underestimate (overestimate) of  $PP_{\text{satellite}}$  for the Western North Pacific Subarctic Gyre. Although both methods for estimating PP have a lot of uncertainty or variability, the data acquisition rate for  $PP_{\text{BLOOMS}}$  estimates between March 2005 and July 2006 was approximately 75%, about four times higher than that for  $PP_{\text{satellite}}$  estimates (approximately 20%).

Finally, we compared the seasonal variability in our PP estimates ( $PP_{\text{BLOOMS}}$ ) with that in organic carbon flux as observed by time-series sediment traps at 150, 540 (or 300), 1000, and 4810 m (Fig. 8; organic carbon flux data: Honda, in preparation). The increases in PP estimated in this study (June and July in 2005 and 2006) were evident in increases in organic carbon flux in the mesopelagic and deep layers, although trapping efficiency for organic carbon flux is problematic. When maximum PP of  $\sim 1000 \text{ mg-C m}^{-2} \text{ day}^{-1}$  appeared on the experimental day of 106 (ExD106) (Fig. 8a), organic carbon flux at 150 m also increased without any time-lag (Fig. 8b). This indicates that  $\text{CO}_2$  assimilated in the surface sunlit layer was quickly transported to the ocean interior at station K2, as reported previously (Honda et al., 2006; Honda and Watanabe, 2007). On the other hand, if it can be said that the peak of carbon flux derived from maximum PP on ExD106 in the upper 60 m (Fig. 8a) appeared on ExD119 at 1000 m (Fig. 8d) and on ExD147 at 4810 m (Fig. 8e), sinking velocity between 60 and 1000 m and between 1000 and 4810 m can be estimated to be approximately 72 ( $[1000-60]/[119-106]$ ) and 136  $\text{m day}^{-1}$ , respectively. Estimates of sinking velocity of  $\sim 150 \text{ m day}^{-1}$  in the deep sea and increase of sinking velocity with depth coincided well with previous reports (e.g., Berelson, 2002).

## 5. Concluding remarks

Our results verify that the  $Ed_{555}/Ed_{443}$  ratio observed at the approximate base of the euphotic layer can be used to estimate  $\text{Chl-}a_{\text{int}}$  and primary productivity if appropriate surface PAR and  $\Psi$  values are available. This new method for estimation of primary productivity, modified from that of Honda et al. (2006), should be useful, especially for high-latitude zones where satellite-based  $\text{Chl-}a$  data acquisition is often hampered by clouds or whitecaps. However, it is not clear whether this method can be applied to coastal areas that have high levels of suspended lithogenic particles and colored dissolved organic matter (CDOM). In coastal waters, the  $Ed_{555}/Ed_{443}$  ratio might be affected not only by phytoplankton biomass ( $\text{Chl-}a_{\text{int}}$ ) but

also by these other substances, although they preferentially absorb QI at shorter wavelengths ( $< 400 \text{ nm}$ ; e.g., Oliver et al., 2004). It is noteworthy that moored optical measurements can be successfully deployed using specialized devices for approximately 1 year without significant degradation due to biofouling or instrument malfunctions. Continuing investigations should include concurrent time-series measurements of optical signals that indicate levels of lithogenic suspended particles, CDOM, and carbonate—measurements such as opacity, backscattering, ultraviolet light, and polarization (e.g., Guay and Bishop, 2002)—which will enable us to conduct comprehensive studies of the biological pump.

## Acknowledgements

We deeply appreciate the following colleagues: the officers and crews of R/Vs *Mirai*, *Natsushima*, and *Kairei*, for mooring work and various on-deck operations; marine technicians of Marine Works Japan Co., for chemical analyses such as primary productivity and pigments; Derek Manov, Frank Spada, and Songnian Jiang of UCSB Ocean Physics Laboratory for providing technical support of the optical systems; and Grace Spada Chang of UCSB (now Sea Engineering, Inc.) for valuable comments on draft versions of the manuscript. We also acknowledge Michael P. Bacon and anonymous reviewers. Their constructive comments improved the paper. Support for T.D. Dickey's contributions was provided by the National Science Foundation, the National Ocean Partnership Program, the Woods Hole Oceanographic Institution HiLaTS program, and his Secretary of the Navy/Chief of Naval Operations Chair in Oceanographic Science.

## References

- Abbott, M.R., Brink, K.H., Booth, C.R., Blasco, D., Swenson, M.S., Davis, C.O., Codispoti, L.A., 1995. Scales of variability of bio-optical properties as observed from near-surface drifters. *Journal of Geophysical Research* 100, 13345–13367.
- Abbott, M.R., Richman, J.G., Letelier, R.M., Bartlett, J.S., 2000. The spring bloom in the Antarctic Polar Frontal Zone as observed from a mesoscale array of bio-optical sensors. *Deep-Sea Research II* 47, 3285–3314.
- Banse, K., English, D.C., 1999. Comparing phytoplankton seasonality in the eastern and western Subarctic Pacific and the western Bering Sea. *Progress in Oceanography* 43, 235–288.
- Behrenfeld, M.J., Falkowski, P.G., 1997. Photosynthetic rates derived from satellite-based chlorophyll concentration. *Limnology and Oceanography* 42 (1), 1–20.
- Behrenfeld, M.J., Boss, E., Siegel, D.A., Shea, D.M., 2005. Carbon-based ocean productivity and phytoplankton physiology from space. *Global Biogeochemical Cycles* 19, 1 GB100610.1029/2004GB002299.
- Berelson, W.L., 2002. Particle settling rates increase with depth in the ocean. *Deep-Sea Research II* 49, 237–251.
- Boyd, P.W., Gall, M.P., Silver, M.W., Bishop, J.K.B., 2008. Quantifying the surface-subsurface biogeochemical coupling during the VERTIGO ALOHA and K2 studies. *Deep-Sea Research II* 55 (14–15), 1578–1593.
- Buesseler, K.O., Lamborg, C.H., Boyd, P.W., Lam, P.J., Trull, T.W., Bidigare, R.R., Bishop, J.K.B., Casciotti, K.L., Dehairs, F., Elskens, M., Honda, M.C., Karl, D.M., Siegel, D.A., Silver, M.W., Steinberg, D.K., Valdes, J., Mooy, B.V., Wilson, S., 2007. Revisiting carbon flux through the ocean's twilight zone. *Science* 316, 567–570.
- Buesseler, K.O., Trull, T.W., Steinberg, D.K., Silver, M.W., Siegel, D.A., Saitoh, S., Lamborg, C.H., Lam, P.J., Karl, D.M., Jiao, N.Z., Honda, M.C., Elskens, M., Dehairs, F., Brown, S.L., Boyd, P.W., Bishop, J.K.B., Bidigare, R.R., 2008. VERTIGO (VERTical Transport In the Global

- Ocean): a study of particle sources and flux attenuation in the North Pacific. *Deep-Sea Research II* 55 (14–15), 1522–1539.
- Campbell, J. Comparisons of algorithms for estimating ocean primary production from surface chlorophyll, temperature, and irradiance. *Global Biogeochemical Cycles* 16 (10)10.1029/2001GB001444.
- Chang, G., Honda, M.C., Nencioli, F., 2008. Innovations in optics for coastal and open-ocean mooring applications. *Sea Technology* August, 17–22.
- Chavez, F.P., Strutton, P.G., Friederich, G., Feely, R.A., Feldman, G.C., Foley, D.C., McPhaden, M.J., 1999. Biological and chemical response of the equatorial Pacific Ocean to the 1997–98 El Niño. *Science* 286, 2126–2131.
- Dickey, T., 1991. The emergence of concurrent high-resolution physical and bio-optical measurements in the upper ocean. *Reviews of Geophysics* 29, 383–413.
- Dickey, T., 2001. The role of new technology in advancing ocean biogeochemical research. *Oceanography* 14 (4), 108–120.
- Dickey, T., Marra, J., Stramska, M., Langdon, C., Granata, T., Weller, R., Plueddemann, A., Yoder, J., 1994. Bio-optical and physical variability in the sub-arctic North Atlantic Ocean during the spring of 1989. *Journal of Geophysical Research* 99, 22541–22556.
- Dickey, T., Frye, D., Jannasch, H., Boyle, E., Manov, D., Sigurdson, D., McNeil, J., Stramska, M., Michaels, A., Nelson, N., Siegel, D., Chang, G., Wu, J., Knap, A., 1998a. Initial results from the Bermuda Testbed Mooring Program. *Deep-Sea Research I* 45, 771–794.
- Dickey, T., Marra, J., Sigurdson, D.E., Weller, R.A., Kinkade, C.S., Zedler, E., Wiggert, J.D., Langdon, C., 1998b. Seasonal variability of bio-optical and physical properties in the Arabian Sea: October 1994–October 1995. *Deep-Sea Research II* 45, 2001–2025.
- Dickey, T., Zedler, S., Frye, D., Jannasch, H., Manov, D., Sigurdson, D., McNeil, J.D., Dobeck, L., Yu, X., Gilboy, T., Bravo, C., Doney, S.C., Siegel, D.A., Nelson, N., 2001. Physical and biogeochemical variability from hours to years at the Bermuda Testbed Mooring site: June 1994–March 1998. *Deep-Sea Research II* 48, 2105–2131.
- Dickey, T., Falkowski, P., 2002. Solar energy and its biological–physical interaction in the sea. In: Robinson, A.R., McCarthy, J.J., Rothschild, B.J. (Eds.), *The Sea*, vol. 12. John Wiley, New York, pp. 401–440 (Chapter 10).
- Dickey, T., Moore, C., O-SCOPE Group, 2003. New sensors monitor bio-optical/biogeochemical ocean changes. *Sea Technology* 44, 17–24.
- Dickey, T., Lewis, M., Chang, G., 2006. Optical oceanography: recent advances and future directions using global remote sensing and in situ observations. *Reviews of Geophysics* 44 (1), RG1001, doi:10.1029/2003RG000148.
- Duntley, S.Q., Austin, R.W., Wilson, R.W., Edgerton, W.H., Moran, C.F., 1974. Ocean color analysis. Ref 74–10, Scripps Institution of Oceanography, University of California, San Diego, La Jolla.
- Falkowski, P.G., 1981. Light-shade adaptation and assimilation numbers. *Journal of Plankton Research* 3, 203–216.
- Falkowski, P.G., Raven, J.A., 1997. In: *Aquatic Photosynthesis*. Blackwell Science 288 pp.
- Foley, D., Dickey, T., McPhaden, M., Bidigare, R., Lewis, M., Barber, R., Garside, C., Manov, D., 1998. Longwaves and primary productivity variations in the equatorial Pacific at 0°, 140°W. *Deep-Sea Research II* 44, 1801–1826.
- Gordon, H.R., 1989. Can the Lambert–Beer law be applied to the diffuse attenuation coefficient of ocean water?. *Limnology and Oceanography* 34, 1389–1409.
- Gordon, H.R., Morel, A.Y., 1983. In: *Remote Assessment of Ocean Color for Interpretation of Satellite Visible Imagery: A Review of Lecture Notes on Coastal and Estuarine Study*. Springer, New York 114 pp.
- Guay, C.K.H., Bishop, J.K.B., 2002. A rapid birefringence method for measuring suspended CaCO<sub>3</sub> concentrations in seawater. *Deep-Sea Research I* 49, 197–210.
- Hama, T., Miyazaki, T., Ogawa, Y., Iwakuma, T., Takahashi, M., Otsuki, A., Ichimura, S., 1983. Measurement of photosynthetic production of a marine phytoplankton population using a stable <sup>13</sup>C isotope. *Marine Biology* 73, 31–36.
- Harrison, P.J., 2002. Station Papa time series: insights into ecosystem dynamics. *Journal of Oceanography* 58, 259–264.
- Hashimoto, S., Shimoto, A., 2002. Light utilization efficiency of size-fractionated phytoplankton in the subarctic Pacific, spring and summer 1999: high efficiency of large-sized diatom. *Journal of Plankton Research* 24 (1), 83–87.
- Holm-Hansen, O., Lorenzen, C.J., Holmes, R.W., Strickland, J.D.H., 1965. Fluorometric determination of chlorophyll. *Journal du Conseil International pour l'Exploration de la Mer* 30, 3–15.
- Honda, M.C., 2003. Biological pump in Northwestern North Pacific. *Journal of Oceanography* 59, 671–684.
- Honda, M.C., Imai, K., Nojiri, Y., Hoshi, F., Sugawara, T., Kusakabe, M., 2002. The biological pump in the northwestern North Pacific based on fluxes and major component of particulate matter obtained by sediment trap experiments (1997–2000). *Deep-Sea Research II* 49, 5595–5626.
- Honda, M.C., Kawakami, H., Sasaoka, K., Watanabe, S., Dickey, T., 2006. Quick transport of primary produced organic carbon to the ocean interior. *Geophysical Research Letters* 33, L16603, doi:10.1029/2006GL026466.
- Honda, M.C., Watanabe, S., 2007. Utility of an automatic water sampler to observe seasonal variability in nutrients and DC in the Northwestern North Pacific. *Journal of Oceanography* 63, 349–362.
- Honjo, S., 1996. Fluxes of particles to the interior of the open ocean. In: Ittekkot, V., Schafer, P., Honjo, S., Depetris, P.J. (Eds.), *Particle Flux in the Ocean*, SCOPE 57. John Wiley & Sons, New York, pp. 91–154.
- Ikusima, I., 1967. Ecological studies on the productivity of aquatic plant communities. III. Effect of depth on daily photosynthesis in submerged macrophytes. *Botanical Magazine, Tokyo* 80, 57–67.
- Imai, K., Nojiri, Y., Tsurushima, N., Saino, T., 2002. Time series of seasonal variation of primary productivity at station KNOT (44°N, 155°E) in the sub-arctic western North Pacific. *Deep-Sea Research II* 49, 5395–5408.
- Karl, D.M., Lukas, R., 1996. The Hawaii Ocean Time-series (HOT) program: Background, rationale and field implementation. *Deep-Sea Research II* 43, 129–156.
- Karl, D.M., Michaels, A.F., Bates, N.R., Knap, A., 2001. Building the long-term picture: the US JGOFS time-series programs. *Oceanography* 14 (4), 6–17.
- Kawakami, H., Honda, M.C., 2007. Time-series observation of POC fluxes estimated from <sup>234</sup>Th in the northwestern North Pacific. *Deep-Sea Research I* 54, 1070–1090.
- Kawakami, H., Honda, M.C., Wakita, M., Watanabe, S., 2007. Time-series observation of dissolved inorganic carbon and nutrients in the Northwestern North Pacific. *Journal of Oceanography* 63, 967–982.
- Kinkade, C.S., Marra, J., Dickey, T.D., Weller, R., 2001. An annual cycle of phytoplankton biomass in the Arabian Sea, 1994–1995, as determined by moored optical sensors. *Deep-Sea Research II* 48, 1285–1301.
- Kirk, J.T.O., 1983. In: *Light and Photosynthesis in Aquatic Ecosystems*. Cambridge press, Cambridge 401 pp.
- Kuwahara, V.S., Strutton, P.G., Dickey, T.D., Abbott, M.R., Letelier, R.M., Lewis, M.R., McLean, S., Chavez, F.P., Barnard, A.H., Morris, J.R., 2003. Radiometric and bio-optical measurements from moored and drifting buoys: measurement and data analysis protocols. In: Mueller, J.L., Fargion, G.S., McClain, C.R. (Eds.), *Ocean Optics Protocols for Satellite Ocean Color Sensor Validation, Revision 4, Vol. VI: Special Topics in Ocean Optics Protocols and Appendices*. NASA/TM-2003-21621NASA Goddard Space Flight Center, pp. 35–79.
- Letelier, R.M., Karl, D.M., Abbott, M.R., Flament, P., Freilich, M., Lukas, R., Strub, T., 2000. Role of late winter mesoscale events in the biogeochemical variability of the upper water column of the North Pacific Subtropical Gyre. *Journal of Geophysical Research* 105, 28723–28739.
- Loisel, H., Morel, A., 1998. Light scattering and chlorophyll concentration in case 1 water: a reexamination. *Limnology and Oceanography* 43, 847–858.
- Louanchi, F., Najjar, R.G., 2000. A global monthly climatology of phosphate, nitrate, and silicate in the upper ocean: spring–summer export production and shallow remineralization. *Global Biogeochemical Cycles* 14, 957–977.
- Manov, D., Chang, G., Dickey, T., 2004. Methods for reducing biofouling on moored optical sensors. *Journal of Atmospheric and Oceanic Technology* 21, 957–967.
- Marra, J., Barber, R.T., 2004. Phytoplankton and heterotrophic respiration in the surface layer of the ocean. *Geophysical Research Letters* 31, L09314, doi:10.1029/2004GL019664.
- Oliver, M.J., Schofield, O., Bergmann, T., Glenn, S., 2004. Deriving in situ phytoplankton absorption for bio-optical productivity models in turbid waters. *Journal of Geophysical Research* 109, C07S11, doi:10.1029/2002JC001627.
- Platt, T., 1986. Primary production of the ocean water column as a function of surface light intensity: algorithm for remote sensing. *Deep-Sea Research* 33, 149–163.
- Platt, T., Sathyendra, S., Caverhill, C.M., Lewis, M.R., 1988. Ocean primary productivity and available light: further algorithms for remote sensing. *Deep-Sea Research* 35, 855–879.
- Siegel, D.A., Westberry, T.K., O'Brien, M.C., Nelson, N.B., Michaels, A.F., Morrison, J.R., Scott, A., Caporelli, E.A., Sorensen, J.C., Maritorena, S., Garver, S.A., Brody, E.A., Ubante, J., Hammer, M.A., 2001. Bio-optical

- modeling of primary production on regional scales: the Bermuda BioOptics project. *Deep-Sea Research II* 48, 1865–1896.
- Smith, R.C., Waters, K.J., Baker, K.S., 1991. Optical variability and pigment biomass in the Sargasso Sea as determined using deep-sea optical mooring data. *Journal of Geophysical Research* 96, 8665–8686.
- Shiomoto, A., 2000. Efficiency of water-column light utilization in the subarctic northwestern Pacific. *Limnology and Oceanography* 45, 982–987.
- Stemann Nielsen, E., 1952. The use of radio-active carbon ( $^{14}\text{C}$ ) for measuring organic production in the sea. *Journal du Conseil International pour l'Exploration de la Mer* 18, 117–140.
- Steinberg, D.K., Carlson, C.A., Bates, N.R., Johnson, R.J., Michaels, A.F., Knap, A.H., 2001. Overview of the US JGOFS Bermuda Atlantic Time-series study (BATS): a decade-scale look at ocean biology and biogeochemistry. *Deep-Sea Research II* 48, 1405–1447.
- Suzuki, R., Ishimaru, T., 1990. An improved method for determination of phytoplankton chlorophyll using *N,N*-dimethylformamide. *Journal of Oceanographic Society of Japan* 46, 190–194.
- Takahashi, T., Sutherland, S.C., Sweeny, C., Poisson, A., Metzl, N., Tilbrook, B., Bates, N., Wanninkhof, R., Feely, R.A., Sabine, C., Olafsson, J., Nojiri, Y., 2002. Global sea-air  $\text{CO}_2$  flux based on climatological surface ocean  $p\text{CO}_2$ , and seasonal biological and temperature effects. *Deep-Sea Research II* 49, 1601–1622.
- Taylor, C.D., Howes, B.L., 1994. Effect of sampling frequency on measurements of seasonal primary production and oxygen status in near-shore coastal ecosystems. *Marine Ecology Progress Series* 108, 193–203.
- Vaillancourt, R.D., Marra, J., Barber, R.T., Smith, W.O., 2003. Primary productivity and in situ quantum yields in the Ross Sea and Pacific Sector of the Antarctic Circumpolar Current. *Deep-Sea Research II* 50, 559–578.
- Volk, T., Hoffert, M.I., 1985. Ocean carbon pumps: analysis of relative strengths and efficiencies in ocean-driven atmospheric  $\text{CO}_2$  changes. In: Sundquist, E., Broecker, W.S. (Eds.), *The Carbon Cycle and Atmospheric  $\text{CO}_2$ : Natural Variations Archean to Present*. Geophysical Monograph. AGU, Washington, DC, pp. 99–110.
- Wiggert, J.D., Dickey, T.D., Granata, T.C., 1994. The effect of temporal undersampling on primary production estimates. *Journal of Geophysical Research* 99, 3361–3371.